Journal of Alloys and Compounds 509 (2011) 6200–6205

Contents lists available at ScienceDirect

Journal of Alloys and Compounds

journal homepage: www.elsevier.com/locate/jallcom

Preparation of $CuIn_{1-x}Ga_xS_2$ ($x = 0.5$) flowers consisting of nanoflakes via a solvothermal method

Xiaojuan Liang[a,b], Jiasong Zhong[a], Fan Yang[a], Wei Hua[a], Huaidong Jin[a], Haitao Liu[a,*], Juncai Sun[b], Weidong Xiang[a,*]

[a] College of Chemistry and Materials Engineering, Wenzhou University, Wenzhou, Zhejiang Province 325035, China
[b] Institute of Materials and Technology, Dalian Maritime University, Dalian 116026, China

ARTICLE INFO

Article history:
Received 18 October 2010
Received in revised form 19 February 2011
Accepted 21 February 2011
Available online 1 March 2011

Keywords:
$CuIn_{0.5}Ga_{0.5}S_2$
L-cysteine
Semiconductors
Chemical synthesis
Microstructure

ABSTRACT

$CuIn_{1-x}Ga_xS_2$ ($x = 0.5$) flowers consisting of nanoflakes were successfully prepared by a biomolecule-assisted solvothermal route at 220 °C for 10 h, employing copper chloride, gallium chloride, indium chloride and L-cysteine as precursors. The biomolecule L-cysteine acting as sulfur source was found to play a very important role in the formation of the final product. The diameter of the $CuIn_{0.5}Ga_{0.5}S_2$ flowers was 1–2 μm, and the thickness of the flakes was about 15 nm. The obtained products were characterized by X-ray diffraction (XRD), energy dispersion spectroscopy (EDS), X-ray photoelectron spectroscopy (XPS), field-emission scanning electron microscopy (FESEM), transmission electron microscopy (TEM), high-resolution transmission electron microscopy (HRTEM), selected area electron diffraction spectroscopy (SAED), and UV–vis absorption spectroscopy. The influences of the reaction temperature, reaction time, sulfur source and the molar ratio of Cu-to-L-cysteine (reactants) on the formation of the target compound were investigated. The formation mechanism of the $CuIn_{0.5}Ga_{0.5}S_2$ flowers consisting of flakes was discussed.

1. Introduction

In recent years, the synthesis and properties characterization of nano- and submicron-sized structures have been attracting an increasing interest owing to their theoretical and practical interests [1]. Especially, semiconductor nanocrystals have been studied extensively as their excellent physical and chemical properties [2] and their potential applications on photo-electronic transition devices [3,4], and their optical properties are highly dependent on size and morphology [5]. Copper–Indium–Gallium Sulfide [$CuIn_{1-x}Ga_xS_2$ ($0 < x < 1$)] is an important quaternary I-III-VI_2 semiconductor material which has a potential for optoelectronics devices [6]. The energy gap (Eg) of $CuIn_{1-x}Ga_xS_2$ can be controlled from 1.5 eV ($CuInS_2$) to 2.49 eV ($CuGaS_2$) by Ga addition [7]. Compared to pure $CuInS_2$ and $CuGaS_2$, $CuGa_{1-x}In_xS_2$ give the advantage of band gap Eg tunability from 1.5 to 2.5 eV [8]. Up to now, there are only a few reports on the synthesis of $CuIn_{1-x}Ga_xS_2$ nanocrystals [6,9]. Nevertheless, these methods generally require rigorous experimental conditions, high reaction temperature, intricate materials, which makes production in large scale difficult. Therefore, a simple, rapid and environment-friendly approach for the large-scale preparation of $CuIn_{1-x}Ga_xS_2$ nanostructures is highly desired.

Biomolecule-assisted synthetic route has been received considerable attention due to biomolecule's special structures and fascinating self-assembling functions and important technological applications in the preparation of inorganic materials [10–13]. Based on these facts, biomolecule-assisted synthesis methods have been new and promising focus on preparation of various nanomaterials where biomolecules have been exploited as the template and reagent [14,15]. In the current work, a small biomolecule, L-cysteine [$HSCH_2CH(NH_2)$–COOH] served as the sulfide source in the formation of $CuIn_{1-x}Ga_xS_2$ nanostructures, which has attracted researchers' attention because of its simple hydrosulfide-group-including structure [16]. To the best of our knowledge, there are no reports about the biomolecule-assisted synthesis of $CuIn_{1-x}Ga_xS_2$ flowers or other forms of structures. Therefore, we report for the first time a solvothermal method for the synthesis of high quality $CuIn_{1-x}Ga_xS_2$ flowers with the assistance of L-cysteine. A possible reaction as well as growth mechanism for the formation of $CuIn_{1-x}Ga_xS_2$ flowers is also proposed.

2. Experimental

2.1. Materials

Copper chloride ($CuCl_2 \cdot 2H_2O$), gallium chloride($GaCl_3$), indium chloride ($InCl_3$) and L-cysteine ($C_3H_7NO_2S$) were purchased from Sinopharm Chemical Reagent Co., Ltd. (Shanghai, China). N,N-dimethylformamide (DMF) were purchased from Shang-

* Corresponding authors. Tel.: +86 577 86596013; fax: +86 577 86689644.
E-mail addresses: lht@wzu.edu.cn (H. Liu), weidongxiang@yahoo.com.cn (W. Xiang).

0925-8388/$ – see front matter © 2011 Elsevier B.V. All rights reserved.
doi:10.1016/j.jallcom.2011.02.117

hai Chemical Reagent Co., Ltd. (Shanghai, China). All the chemical reagents used in the experiments were analytical grade and used without further purification. Double distilled water was used throughout the experiments.

2.2. Synthesis of the $CuIn_{0.5}Ga_{0.5}S_2$ flowers

In a typical process, 1 mmol $CuCl_2{\cdot}2H_2O$, 0.5 mmol $GaCl_3$, 0.5 mmol $InCl_3$, and 2 mmol L-cysteine were dissolved in 40 mL DMF under vigorous stirring for 10 min to obtain a clear solution. Then the clear solution was transferred into a 50 mL Teflon-lined stainless-steel autoclave with a filling capacity of 80% of the total volume. The autoclave was sealed and maintained at 220 °C for 10 h, and then naturally cooled to room temperature. After the reaction, the resulting precipitate was centrifuged and washed with distilled water and absolute ethanol several times, and then dried in a vacuum at 55 °C for 4 h.

2.3. Characterization

The structure and phase purity of the as-prepared samples was characterized by powder X-ray diffraction patterns equipped with graphite monochromator Cu Kα radiation (λ = 1.5406 Å) at 40 kV and 40 mA, and X-ray photoelectron spectroscopy (XPS) analysis was performed on an ESCALAB 250 X-ray photoelectron spectroscopy using Monochrome Al Ka as the excitation source. The morphology of the as-synthesized powders analysed by field-emission scanning electron microscope (FESEM, JEOL-6700F, Accelerating voltage of 10 kV) with energy-disperse X-ray spectroscopy (EDS) attachment. The transmission electron microscopy (TEM) images, high-resolution TEM (HRTEM) and selected area electron diffraction (SAED) images were recorded on a FEI Tecnai F-20 transmission electron microscopy at an acceleration voltage of 200 kV. UV–vis absorption spectra were recorded on an UV-2501PC spectrophotometer.

3. Results and discussion

The typical XRD pattern of the product prepared in DMF at 220 °C for 10 h was shown in Fig. 1. It shows that the most intense peak at $2\theta = 28.48°$ is attributed to the chalcopyrite phase oriented along the (1 1 2) tetragonal crystal plane. The XRD patterns are consistent with the tetragonal phases $CuInS_2$ (JCPDS No. 75-0106) and $CuGaS_2$ (JCPDS No. 82-1531). No impurity phases are detected from this pattern, confirming that the product obtained is composed of the pure $CuIn_{0.5}Ga_{0.5}S_2$ crystals. The strong and sharp peaks indicate that the as-prepared $CuIn_{0.5}Ga_{0.5}S_2$ is well crystallized.

The morphology of the $CuIn_{0.5}Ga_{0.5}S_2$ powders synthesized at 220 °C for 10 h via biomolecule-assisted solvothermal method was observed by field-emission scanning electron microscopy (FESEM) and illustrated in Fig. 2. Fig. 2a and b shows a typical low-magnification FESEM micrograph of the $CuIn_{0.5}Ga_{0.5}S_2$ powders. It can be seen in Fig. 2a and b, the as-prepared $CuIn_{0.5}Ga_{0.5}S_2$ powders are consisted of large-scale flowers with the diameter about 1–2 μm. High-magnification FESEM micrograph of the $CuIn_{0.5}Ga_{0.5}S_2$ powders is represented in Fig. 2c that depicts the surface morphology of the single flower. The $CuIn_{0.5}Ga_{0.5}S_2$ flowers are composed of nanoflakes with the thickness of a single flake is about 15 nm. The chemical compositions of the as-prepared $CuIn_{0.5}Ga_{0.5}S_2$ flowers were investigated by energy dispersion spectroscopy (EDS). Only peaks of the elements Cu, In, Ga and S are present in the EDS spectrum (Fig. 2d). The atomic ratio of Cu, In, Ga, and S is about 2.04:1:0.97:3.97, which is close to the stoichiometric composition of $CuIn_{0.5}Ga_{0.5}S_2$.

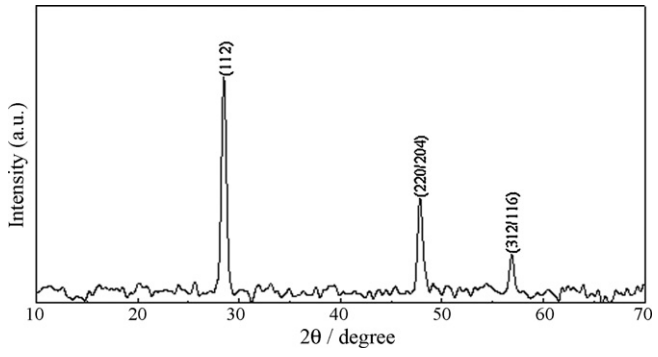

Fig. 1. Typical XRD pattern of as-prepared $CuIn_{0.5}Ga_{0.5}S_2$ synthesized at 220 °C for 10 h.

The states of elements and composition information about as-prepared $CuIn_{0.5}Ga_{0.5}S_2$ sample were further determined by the XPS technique. The survey spectrum results show the presence of Cu, In, Ga and S, as well as C from reference and O impurity (figure not show here). Oxygen in the sample is likely due to exposure to the atmosphere since nanocrystalline material exhibits a high surface area-to-volume ratio [17]. In order to determine the valency state and atomic ratio, high-resolution spectra were also taken for the Cu2p region, the In3d region, the Ga2p region and the S2p region. The Cu2p core level spectrum is shown in Fig. 3a, indicating that the observed values of the binding energies for $Cu2p_{3/2}$ and $Cu2p_{1/2}$ are about 931.75 and 951.65 eV, respectively, which are in agreement with the literature values for Cu^+ [18]. In addition, the $Cu2p_{3/2}$ satellite peak of Cu^{2+} which is usually located at 942 eV [19] does not appear in the spectrum. Therefore, it can be concluded that only Cu^+ exists in the sample. The In3d core-level spectra region (Fig. 3b) indicates that the binding energy for $In3d_{5/2}$ (444.51 eV) and $In3d_{3/2}$(452.16 eV) are in good agreement with the report values for In^{3+} [20]. The Ga2p core-level spectra region (Fig. 3c) provides the binding energy for $Ga2p_{3/2}$ (1117.94 eV) and $Ga2p_{1/2}$(1144.91 eV), which are close to the respective values for Ga^{3+}. The S2p core level spectrum (Fig. 3d) shows a peak located at 161.8 eV, which is also in agreement with the literature [21]. Hence, the XPS analysis is consistent with the valence states for $CuIn_{0.5}Ga_{0.5}S_2$ flowers being Cu^+, In^{3+}, Ga^{3+} and S^{2-}. No obvious impurities could be detected in the sample, indicating that the level of impurities is lower than the resolution limit of XPS (1 at.%). The intensities of the relevant peaks gave the sample's surface stoichiometry of Cu/In/Ga/S of 2.11:1:0.96:3.89, in good agreement with the XRD and EDS results.

The structure and morphology of the as-prepared samples were further examined by transmission electron microscopy (TEM). Typical TEM images of the sample are given in Fig. 4a and b. It can be seen from the images that the synthesized $CuIn_{0.5}Ga_{0.5}S_2$ crystals appeared to display uniform flowers morphology with an average dimensions of about 1–2 μm in diameter. The higher-magnification TEM image (Fig. 4b) suggests that the flower contains many flakes, confirming the above FESEM observations. It is difficult to get HRTEM and SAED images of the complete flowers because it is too thick to be penetrated by electron beam. The fringe of single flower was investigated (area marked with an ellipse in Fig. 4b). The SAED pattern (Fig. 4c) is agreed well with the poly-crystalline nature of the $CuIn_{0.5}Ga_{0.5}S_2$ crystals. These diffraction circles can be resolved into three distinct planar systems with identical planar spacing, which are caused by the (1 1 2), (2 2 0/2 0 4) and (3 1 2) crystal planes, respectively. The HRTEM image (Fig. 4d) of the $CuIn_{0.5}Ga_{0.5}S_2$ product shows that the lattice fringes are separated by 0.313 nm, which matches the spacing distance of (1 1 2) planes of chalcopyrite $CuIn_{0.5}Ga_{0.5}S_2$ (d(1 1 2) = 0.3141 nm).

To fully understand the effect of reaction temperature on the microstructure and morphology of the synthesized samples, FESEM examination was conducted. Fig. 5 shows the FESEM images of the products synthesized at different temperatures for 10 h. It was found that temperature significantly affected the shape of the products. When the product obtained at 160 °C for 10 h, some flakes and large number of irregular particle are coexist in the sample (Fig. 5a). When the reaction temperature increased to 180 °C, the sample mainly contains of flake shapes and some irregular particles (Fig. 5b). With a reaction temperature of 200 °C, a large number of flower consist of nanoflakes and some single nanoflakes are observed, and the thickness of nanoflakes is about 10 nm (Fig. 5c). When the reaction temperature was increased to 220 °C, uniform

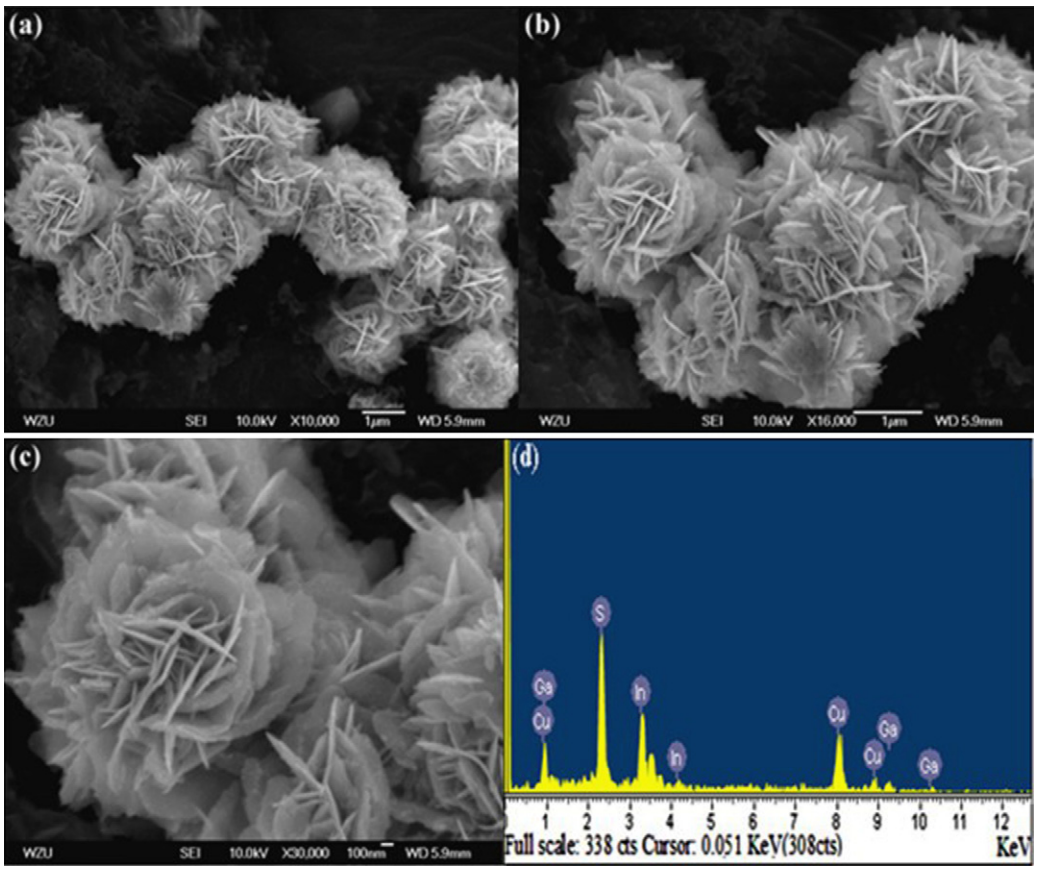

Fig. 2. (a–c) FESEM images of the $CuIn_{0.5}Ga_{0.5}S_2$ and (d) EDS spectrum of a single flake.

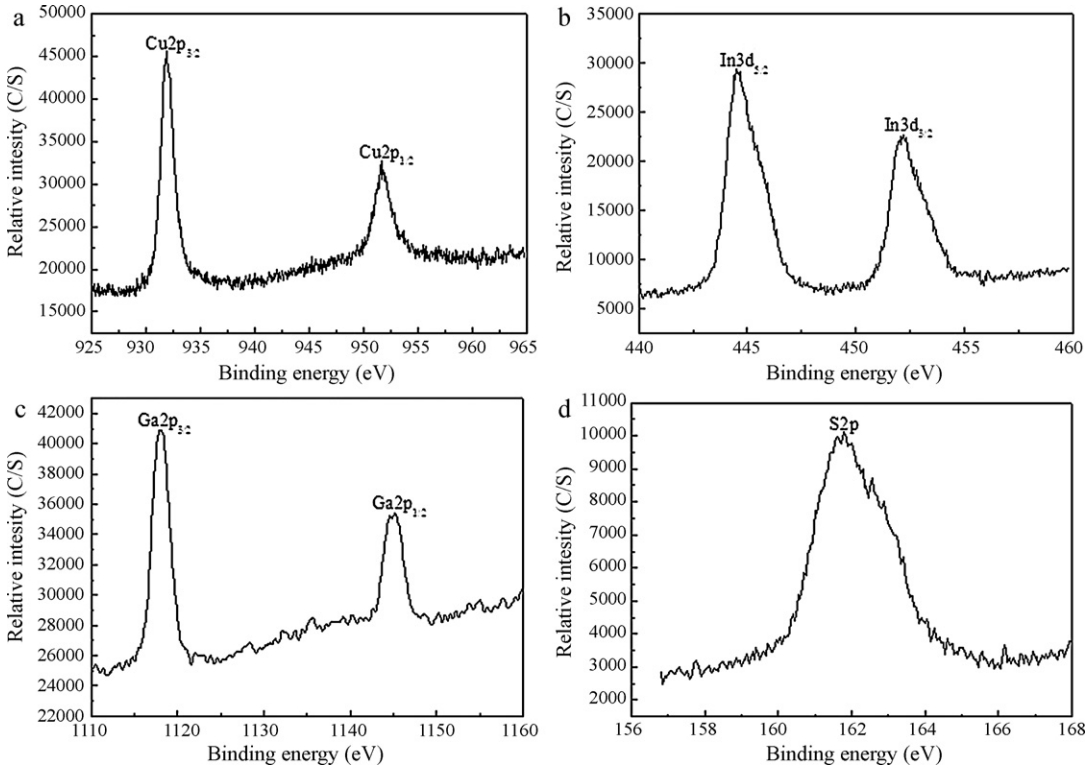

Fig. 3. XPS spectra of as-prepared $CuIn_{0.5}Ga_{0.5}S_2$ sample in DMF: (a) Cu core level spectrum, (b) In core level spectrum, (c) Ga core level spectrum, and (d) S core level spectrum.

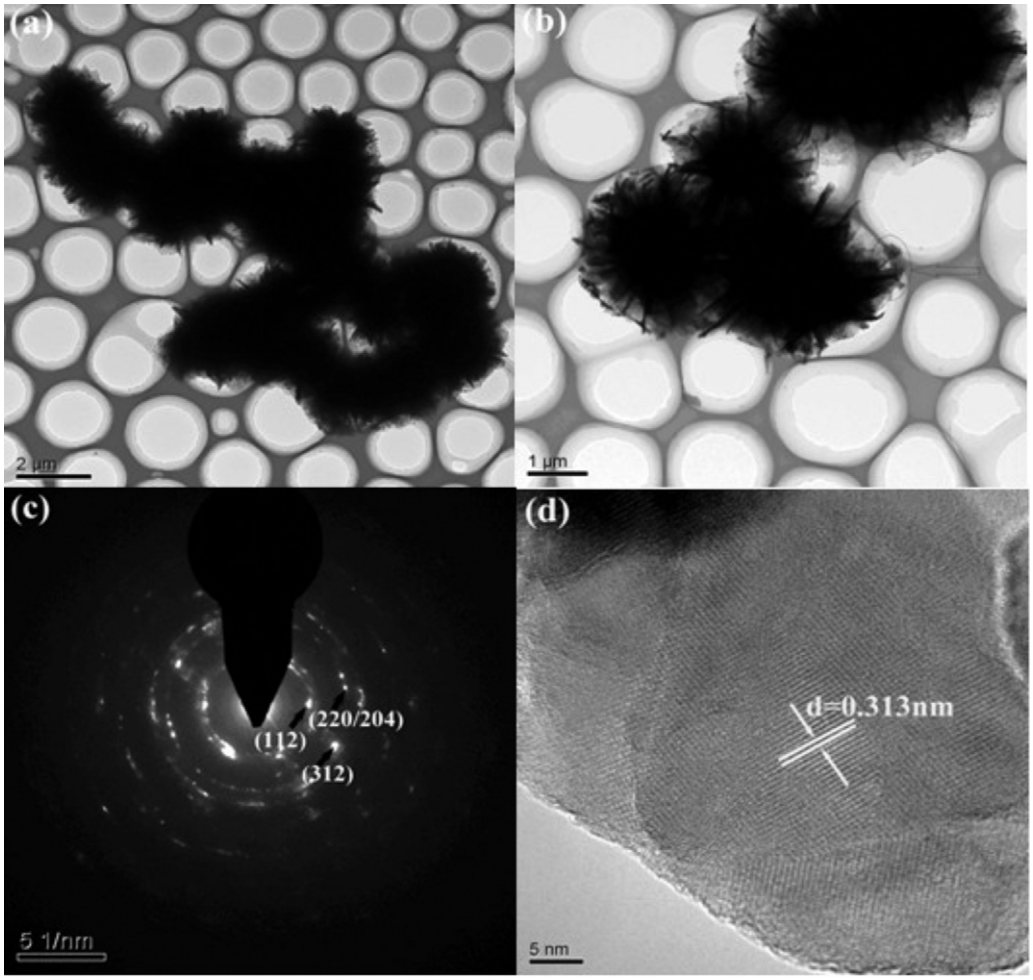

Fig. 4. (a and b) TEM image of the $CuIn_{0.5}Ga_{0.5}S_2$ product, (c) SAED image of the fringe of individual $CuIn_{0.5}Ga_{0.5}S_2$ flower, (d) HRTEM image of the $CuIn_{0.5}Ga_{0.5}S_2$ product.

flower with nanoflakes were obtained (Fig. 2a–c), and the thickness of nanoflakes is about 15 nm (Fig. 5c). However, when the reaction temperature was further increased to 240 °C, the sample mainly remains as flower shapes and the diameter of nanoflakes become thicker on the surface of the flower (Fig. 5d). According to the above analysis, we can conclude that the suitable reaction temperature was ranged from 200 °C to 240 °C. At a suitable temperature, longer treatment time (10–15 h) did not significantly affect the crystallinity or the yields of the target products.

It is noteworthy that the molar ratio of $CuCl_2$ and L-cysteine apparently had a significant effect on the formation of the current morphology. When we decrease the molar ratio of $CuCl_2$ and L-cysteine from 1:2 to 1:1 while other conditions remain unchanged (compared with the condition of Fig. 2), the product is $CuIn_{0.5}Ga_{0.5}S_2$ flower with irregular flakes and some irregular particles, as shown in Fig. 6a. When the molar ratio of $CuCl_2$ and L-cysteine in the reacting mixture is increased to 1:3, novel snowflake-like could be obtained, and their typical FESEM image is shown in Fig. 6b, from which it can be clearly seen that these snowflake-like are comprised of many flakes with an irregular arrangement. The morphology of the products is obviously different from the structure of the above-mentioned products in Fig. 2. Therefore, we think the concentration of L-cysteine is very important to the formation of $CuIn_{0.5}Ga_{0.5}S_2$ flowers.

It is also worth mentioning here that sulfur sources have great effects on the final morphologies of $CuIn_{0.5}Ga_{0.5}S_2$ crystal. And some experiments have carried out to conform whether the nanoflowers are motivated by the presence of L-cysteine or by the strong contribution of DMF. In order to investigate the influence of solvent condition on the morphology of $CuIn_{0.5}Ga_{0.5}S_2$ sample, reactions are carried out with the distilled water replace DMF as the solvent while other conditions were constant. When using distilled water as the solvent, regular microspheres with some flakes are obtained (Fig. 6c). The influences of sulfur source on the morphology and microstructure of the products are also investigated. When thiourea is used as the sulfur source while other conditions remain unchanged, irregular flakes are obtained (Fig. 6d). And other experiments are also carried out. Based on the above experimental results, we can know that the nanoflowers are motivated by the presence of L-cysteine.

The UV–vis absorption spectra of the as-prepared $CuIn_{0.5}Ga_{0.5}S_2$ flower have been measured at room temperature and are shown in Fig. 7. The absorption spectra of $CuIn_{0.5}Ga_{0.5}S_2$ flowers, typically showing a broad shoulder with a trail in the long-wavelength direction, can be tuned to cover the whole visible region. This result is close to the literature data [9].

The exact mechanism for the formation of $CuIn_{0.5}Ga_{0.5}S_2$ flower with a large number of nanoflakes is still unclear. The possible formation mechanism for nanoflowers was proposed according to the foregoing experimental results and relative Refs. [22–25]. Firstly, since the temperatures reached are certainly high enough to melt indium and Gallium under the solvothermal process, and CuInxGay alloy is formed. Secondly, the new form CuInxGay alloy is transformed to $CuInxGayS_2$ nuclei under sulfuration by the thiol

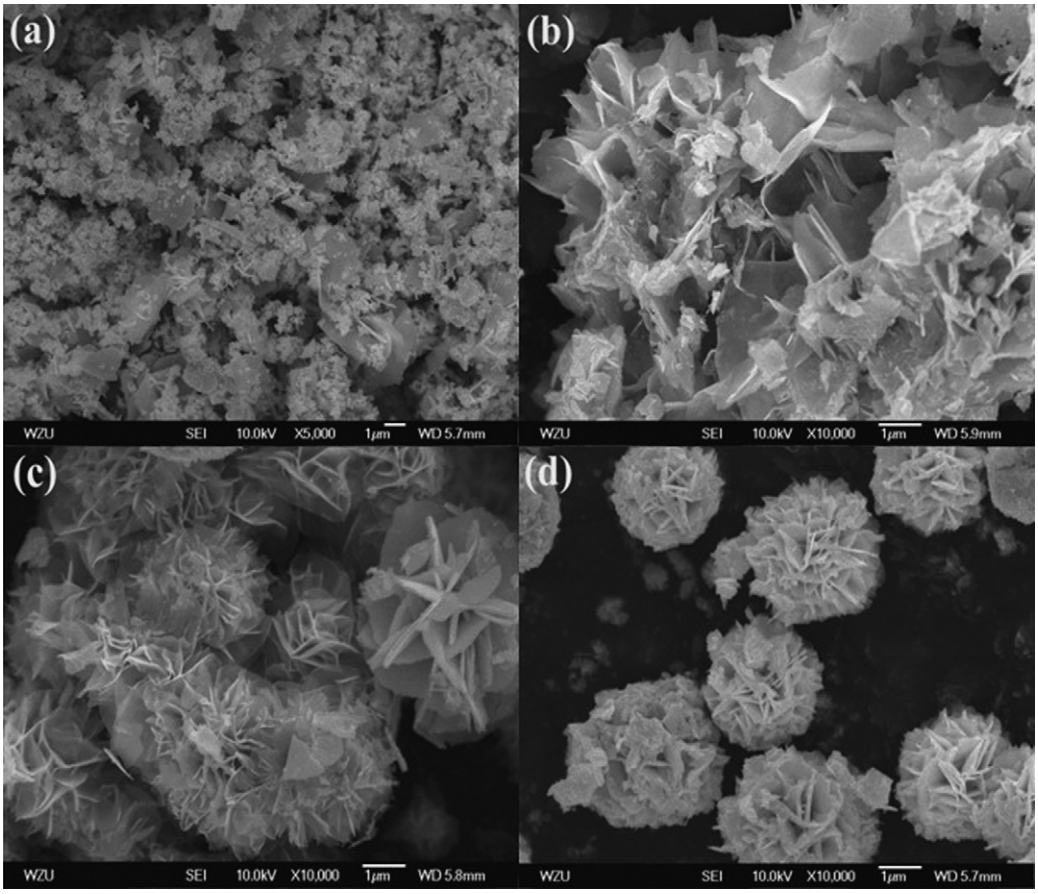

Fig. 5. FESEM images of the $CuIn_{0.5}Ga_{0.5}S_2$ powders synthesized at different temperatures for 10 h: (a) 160 °C, (b) 180 °C, (c) 200 °C, and (d) 240 °C.

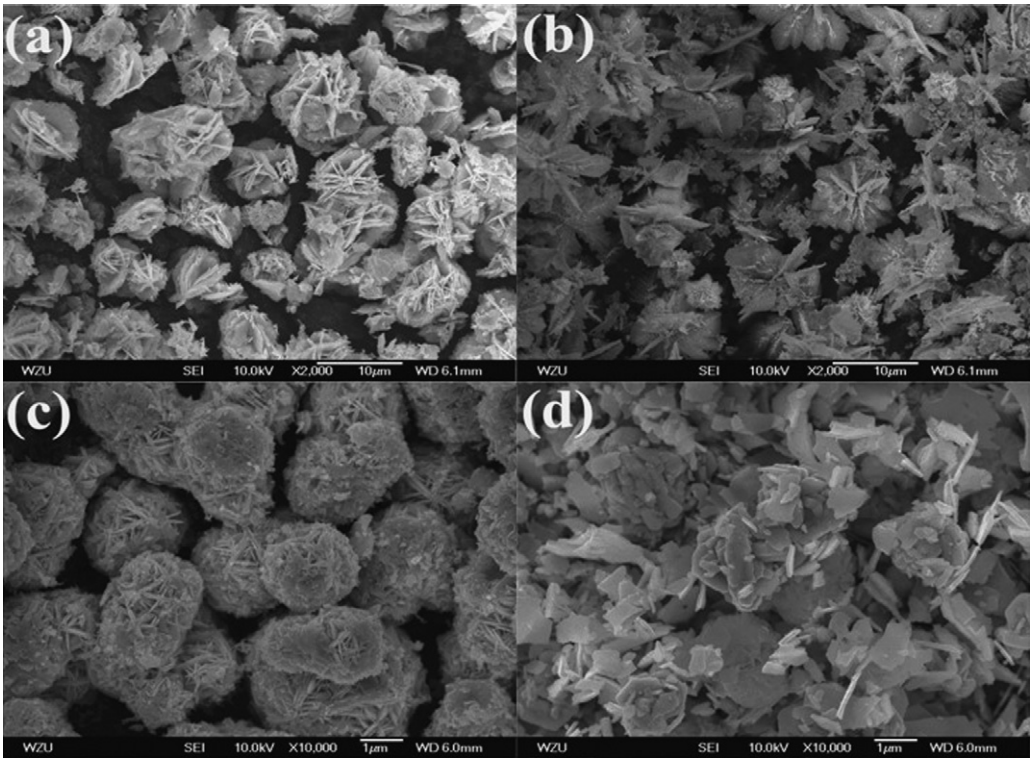

Fig. 6. FESEM images of $CuIn_{0.5}Ga_{0.5}S_2$ prepared at various molar ratios of $CuCl_2$ and L-cysteine: (a) 1:1 and (b) 1:3; FESEM images of $CuIn_{0.5}Ga_{0.5}S_2$ obtained under different conditions, (c) using distilled water as the solvent, and (d) using thiourea as the sulfur source while keep other reaction conditions constant.

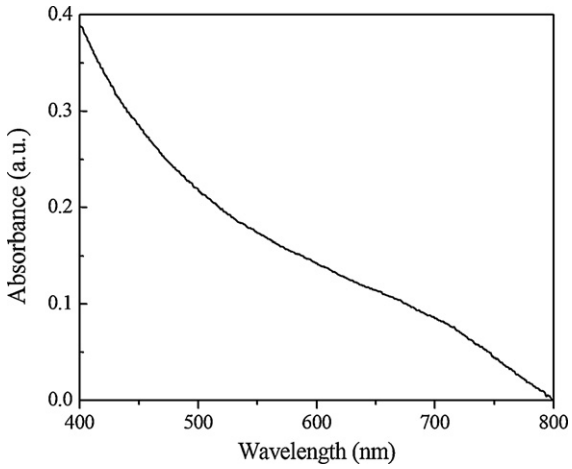

Fig. 7. UV–vis absorption spectra of $CuIn_{0.5}Ga_{0.5}S_2$ powders prepared at 220 °C for 10 h.

groups –SH provided by decomposed L-cysteine since this amino acid decomposes around 240 °C at normal pressure. A possible formation mechanism of $CuIn_xGa_yS_2$ ($x = y = 0.5$) nuclei could be formulated as follows:

$$Cu + xIn + yGa \xrightarrow{\Delta} CuIn_xGa_y \xrightarrow{sulfuration} CuIn_xGa_yS_2$$

The initial nuclei rapidly aggregated into flowerlike particles. Then, the flowerlike particles serve as seeds and grow larger. After a period of rapid growth, the concentration of reactants decreased. There is an equation between nucleation and dissolution. At last, with the prolongation of reaction time, the flower-like nanostructures are produced on a large scale at the expense of the small particles. On the surface of these flowers, many nanoflakes are formed because of the oriented growth of L-cysteine-based molecules and the Ostwald ripening process [26,27]. More studies are required to clarify the growth mechanism of these nanocrystals.

4. Conclusions

In summary, $CuIn_{0.5}Ga_{0.5}S_2$ flower with a large number of nanoflakes have been successfully prepared via a mild solvothermal method with L-cysteine as the sulfur source. L-cysteine plays a critical role in the synthesis of $CuIn_{0.5}Ga_{0.5}S_2$ flower. The reaction temperature, reaction time, sulfur source and the molar ratio of Cu-to-L-cysteine (reactants) on the formation of $CuIn_{0.5}Ga_{0.5}S_2$ are investigated. This solvothermal method using L-cysteine as the sulfur source is simple, efficient and it could be used to synthesize other quaternary chalcogenide compounds. XRD, FESEM, EDS, XPS, TEM, HRTEM, SAED and UV–vis are used to characterize the as-prepared sample.

Acknowledgment

The authors acknowledge the financial support from National Natural Sciences Foundation of China (Grants No. 50772075 and 50972107).

References

[1] J.H. Peng, Y.H. Xu, H. Wu, M. Hojamberdiev, Y.H. Fu, J. Wang, G.Q. Zhu, J. Alloys Compd. 490 (2010) L20–L23.
[2] J.T. Hupp, K.R. Poeppelmeier, Science 309 (2005) 2008–2009.
[3] K.F. Li, Q.J. Wang, X.Y. Cheng, T.X. Lv, T.K. Ying, J. Alloys Compd. 504 (2010) L31–L35.
[4] N. Ghows, M.H. Entezari, Ultrason. Sonochem. 18 (2011) 269–275.
[5] M. Xue, X.H. Zhang, X. Wang, B. Tang, Mater. Lett. 64 (2010) 1357–1360.
[6] T. Kato, T. Omata, T. Nakamura, D. Anno, Y. Nabetani, T. Matsumoto, J. Cryst. Growth 275 (2005) e531–e536.
[7] F.M. Courtel, A. Hammami, R. Imbeault, G. Hersant, R.W. Paynter, B. Marsan, M. Morin, Chem. Mater. 22 (2010) 3752–3761.
[8] P.S. Vasekar, A.H. Jahagirdar, N.G. Dhere, Thin Solid Films 518 (2010) 1788–1790.
[9] C. Sun, J.S. Gardner, G. Long, C. Bajracharya, A. Thurber, A. Punnoose, R.G. Rodriguez, J.J. Pak, Chem. Mater. 22 (2010) 2699–2701.
[10] J.H. Jiang, R.L. Yu, R. Yi, W.Q. Qin, G.Z. Qiu, X.H. Liu, J. Alloys Compd. 493 (2010) 529–534.
[11] J.Q. Jiao, X. Liu, W. Gao, C.W. Wang, H.J. Feng, X.L. Zhao, L.P. Chen, Solid State Sci. 11 (2009) 976–981.
[12] J.S. Zhong, J. Hu, W. Cai, F. Yang, L.J. Liu, H.T. Liu, X.Y. Yang, X.J. Liang, W.D. Xiang, J. Alloys Compd. 501 (2010) L15–L19.
[13] T. Douglas, D.P.E. Dichson, S. Betteridge, J. Charnoch, C.D. Garner, S. Mann, Science 269 (1995) 54–57.
[14] J.Q. Jiao, L.P. Chen, X. Liu, W. Gao, H.J. Feng, Mater. Res. Bull. 44 (2009) 1161–1165.
[15] X.F. Qu, G.T. Zhou, Q.Z. Yao, S.Q. Fu, J. Phys. Chem. C 114 (2010) 284–289.
[16] B. Zhang, X.C. Ye, W.Y. Hou, Y. Zhao, Y. Xie, J. Phys. Chem. B 110 (2006) 8978–8985.
[17] D. Chen, G.Z. Shen, K.B. Tang, X.M. Liu, Y.T. Qian, G.E. Zhou, J. Cryst. Growth 253 (2003) 512–516.
[18] J. Llanos, A. Buljan, C. Mujica, R. Ramirez, J. Alloys Compd. 234 (1996) 40–42.
[19] L.D. Partain, R.A. Schneider, L.F. Donaghey, P.S. Mcleod, J. Appl. Phys. 57 (1985) 5056–5066.
[20] X.H. Xu, F. Wang, J.J. Liu, K.C. Park, M. Fujishige, Sol. Energy Mater. Sol. Cells 95 (2011) 791–796.
[21] C.D. Wagner, W.M. Riggs, L.E. Davis, J.F. Moulder, G.E. Muilenberg, Handbook of X-ray Photoelectron Spectroscopy, Perkin-Elmer Corp, Eden Prairie, MN, 1978.
[22] C.C. Landry, J. Lockwood, A.R. Barron, Chem. Mater. 7 (1995) 699–706.
[23] G.S. Chen, J.C. Yang, Y.C. Chan, L.C. Yang, W. Huang, Sol. Energy Mater. Sol. Cells 93 (2009) 1351–1355.
[24] W. Liu, J.G. Tian, Q. He, F.Y. Li, C.J. Li, Y. Sun, Thin Solid Films 519 (2010) 244–250.
[25] C.Y. Su, W.H. Ho, H.C. Lin, C. YoNieh, S.C. Liang, Sol. Energy Mater. Sol. Cells 95 (2011) 261–263.
[26] B. Li, G. Rong, Y. Xie, L. Huang, C. Feng, Inorg. Chem. 45 (2006) 6404–6410.
[27] S.J. Bao, Q.L. Bao, C.M. Li, T.P. Chen, C.Q. Sun, Z.L. Dong, Y. Gan, J. Zhang, Small 3 (2007) 1174–1177.